Saudi Pharmaceutical Journal 27 (2019) 738–752

Contents lists available at ScienceDirect

Saudi Pharmaceutical Journal

journal homepage: www.sciencedirect.com

An alternative approach to wound healing field; new composite films from natural polymers for mupirocin dermal delivery

Neslihan Üstündağ Okur [a,*], Nesrin Hökenek [b], Mehmet Evren Okur [c], Şule Ayla [d], Ayşegül Yoltaş [e], Panoraia I. Siafaka [b,f], Erdal Cevher [g]

[a] University of Health Sciences, Faculty of Pharmacy, Department of Pharmaceutical Technology, Istanbul, Turkey
[b] Istanbul Medipol University, School of Pharmacy, Department of Pharmaceutical Technology, Istanbul, Turkey
[c] University of Health Sciences, Faculty of Pharmacy, Department of Pharmacology, İstanbul, Turkey
[d] Istanbul Medipol University, School of Medicine, Department of Histology and Embryology, Beykoz, Istanbul, Turkey
[e] Ege University, Faculty of Science, Department of Biology, Fundamental and Industrial Microbiology Division, Bornova, Izmir, Turkey
[f] Aristotle University of Thessaloniki, Department of Chemistry, Thessaloniki, Greece
[g] Istanbul University, Faculty of Pharmacy, Department of Pharmaceutical Technology, Istanbul, Turkey

ARTICLE INFO

Article history:
Received 24 January 2019
Accepted 19 April 2019
Available online 20 April 2019

Keywords:
Chitosan
Sodium alginate
Mupirocin
Dermal delivery
Wound healing
In vivo

ABSTRACT

In this study, novel adhesive films were prepared for Mupirocin dermal delivery. Natural polymers as chitosan, sodium alginate and carbopol were used for films development to evaluate possible interactions and drug release properties. Solvent evaporation method was used for films preparation. Preliminary studies involved FT-IR spectroscopy and Scanning Electron Microscopy to specify interactions and morphology. Thickness, tensile strength and water uptake in phosphate buffer saline were evaluated whereas *in vitro* release studies were also performed. *In vitro* drug release studies demonstrated that mupirocin release was improved. *Ex vivo* bioadhesion and permeation studies using Balb-c mice were performed to check the suitability of the films. Antimicrobial ability was evaluated by agar well diffusion tests. Finally, excisional wound model applied to test the wound healing effect and evaluated macroscopic and histopathologically. One formulation was found more effective compared to the market product for wound healing at Balb-c mice.

1. Introduction

Until now wound healing is still an unmet challenge among surgical society. In fact, wounds introduced by chronic diseases, burns and post-operative traumas can be fatal in many cases since they can be colonized easily by resistant bacteria and microbes. Although, nowadays, patients can survive massive burns which once were fatal most of these patients develop hypertrophic scars decreasing their quality of life and delaying reintegration into society (Finnerty et al., 2016). On the other hand, the 96% of the 300.000 recorded burn incidents could be fatal or at least life-threatening for patients due to undesirable complications (Khalid et al., 2017; Siafaka et al., 2016d). Last decades, an improvement on outcomes for severely burned patients have been attributed due to advances in modern medical care in specialized burn centers. However, wound infection is a quite important problem for clinicians and requires immediate and intensive special care (Cambiaso-Daniel et al., 2018). Several factors (obesity, age, congenital diseases) rise the risk of developing wound infection, and individuals who sustain a severe burn have a particularly high risk for wound sepsis. Invasive wound infection and secondary sepsis incidences can be minimized via early excised the eschar but it has been reported that most deaths in severely burn-injured patients occured due to burn wound sepsis or complications due to inhalation injury (Cambiaso-Daniel et al., 2018). Numerous dressings were prepared so as to cover the wound surface in order to create desirable area for epidermal regeneration and act as proper obstacle against injury infection and water decrement (Khalid et al., 2017). Wound healing is the process composed of healing of dermal and epidermal tissues by their regeneration. It involves consecutive cascade of stages inflammation, migration,

* Corresponding author.
E-mail address: neslihanustundag@yahoo.com (N. Üstündağ Okur).
Peer review under responsibility of King Saud University.

Production and hosting by Elsevier

https://doi.org/10.1016/j.jsps.2019.04.010
1319-0164/

proliferation, and maturation (Kataria et al., 2014). In addition, wound healing involved cell-cell and cell-matrix interactions which proceed in three overlapping phase's viz. inflammation (0–3 days), cellular proliferation (3–12 days) and remodeling (3–6 months) (Üstündag-Okur et al., 2014).

It has been reported that wound healing processed naturally on its own, however, sepsis, disruption of tissue and skin layer, maggot's formation, extension of infection to adjacent and interior organs complicate the process (Hima Bindu et al., 2010). Many wound dressings are loaded with antimicrobial agents or healing agents which can prophylactic act against infectious organisms and prevent incidents as sepsis etc (Henry et al., 2014; Siafaka et al., 2016d).

Topical antibiotics can play an important role to prevent and to treat of many main dermal bacterial infections mostly seen in dermatological practice like localized superficial infections due to surgery, injury, and abrasion (Mpharm et al., 2010). Mupirocin is an antibacterial agent which effectively used, against wound pathogens including MRSA, as topical ointment to treat various topical wounds such as burns and foot ulcers because of its effectiveness (Perumal et al., 2014).

Hydrogel dressings are of great interest because they produce an ideal hydration environment for healing (Mohamad et al., 2014; Yasasvini et al., 2017). They present low interfacial tension, high molecular and oxygen permeability, good moisturizing and mechanical properties that resemble physiological soft tissue (Yasasvini et al., 2017). For these reasons, polysaccharides which have hydrogel forming properties criticized as advantageous as a wound dressing material (Raval et al., 2011; Siafaka et al., 2016d). Hydrogels are three-dimensional cross-linked polymeric networks, assessed as highly biocompatible or biodegradable and applied effectively as controlled drug delivery and wound healing systems. It is usually referred that the optimum wound should mimic many properties of human skin. In further, it should possesses adhesiveness, elasticity, durability, and should be occlusive and impermeable to bacteria. Chitosans are good candidates for wound healing activity because of their biocompatibility, ability to absorb exudates, and film forming properties (Alsarra, 2009).

Chitin and chitosan have been proposed as biomaterials, which applied in biomedical and industrial field due to their potential as antimicrobial activity and stimulation of healing (Murakami et al., 2010; Siafaka et al., 2015; Siafaka et al., 2016d). Chitosan (CS) is also known to promote drainage, prevent the buildup of exudates, and may serve as bed for autografting in wound therapy. Moreover, it promotes gas exchange, essential in wound healing process (Dai et al., 2011; Hurler et al., 2012; Inukai et al., 2013; Murakami et al., 2010; Pawar et al., 2013; Sezer et al., 2007; Zhou et al., 2017). Alginate is an anionic polysaccharide, which is capable to form hydrogels under very mild conditions, at 25 °C. Alginate has been commonly evaluated due to its biocompatibility, biodegradability, relative low cost, low toxicity and gelling properties (Kurczewska et al., 2017; Li et al., 2017; Murakami et al., 2010; Pereira et al., 2013). Carbopol is a hydrophilic, mucoadhesive, biocompatible crosslinked polymer of polyacrylic acid. It has been used in biomaterials as wound dressings, topical and transdermal (Grip et al, 2017; Singh et al., 2013).

In this study, hydrogel films containing chitosan, sodium alginate and combination of them with carbopol were used in order to effectively be applied as wound healing promoters. Chitosan was chosen due to its favorable property to act as wound healing and antimicrobial agent, as well as its ability to produce hydrogel like films which are essential as wound dressing. Sodium alginate was selected as film matrix since there are no many studies of sodium alginate solvent castings films and also due to its low toxicity and cost can be a favorable dermal film. Additionally, by blending chitosan and sodium alginate, authors aimed to improve properties of the each polysaccharide. However, this was not achieved. In further, carbopol was added in order to enhance mucoadhesiveness of the gelling system since it is intended to be used in dermal delivery. Mupirocin antibiotic was loaded so as to improve antimicrobial ability of the developed films. Finally, the aim of this study was to prepare a novel wound dressing system with enhanced antibacterial and wound healing activity so as to prevent severe infection of the wound which can lead to undesirable effects such as bacteraemia and/or sepsis and multiple organ failure.

2. Materials and methods

2.1. Materials

MUP was generously gifted from Pharmactive Pharmaceuticals Company, Turkey. Chitosan (medium Mw, deacetylation degree: 75–85%), sodium alginate and propylene glycol were purchased from Sigma, Germany. Carbopol and Glycerine were purchased from Doga Ilac Pharmaceuticals Company, Turkey. PEG 400, Nutrient agar and methanol were obtained from Merck, Germany. All the other chemicals and solvents were of analytical or HPLC grade.

2.2. Preparation of composite films

The formulations were developed by solvent casting technique (Priyadarshi et al., 2018; Tanwar, 2005). Chitosan (CS) and sodium alginate (SA) were prepared separately and mixed with or without carbopol in different proportions to prepare film formulations using a magnetic stirrer. Glycerin, propylene glycol or PEG 400 at the range of 5%–20% were used as plasticizers. For CS dissolution, since it is insoluble in water, acidic pH was adjusted using 10% v/v lactic acid solution. Distilled water was used as solvent for sodium alginate and carbopol solutions. After the prepared formulations were supplemented to 30 mL with solvent of polymer which was used in the formulation, they were poured into petri dishes and the meat was dried at 40 °C for 48 h.

2.2.1. Preparation of MUP loaded films

Mupirocin was added after the formulation was prepared, corresponding to 2% of the total weight of the formulation.

2.3. Characterization of polymer films

2.3.1. Thickness

Film thickness is a quite important property considering that can affect the time required to absorb the polymer into the body. The determination of the uniform thickness of each film was done by a screw gauge which was applied at three different sites of the film. The mean thickness is calculated (Hima Bindu et al., 2010).

2.3.2. Moisture loss

Moisture loss was studied by the following method: Firstly, the films were weighed separately and kept in a desiccators containing fused calcium chloride at RT for 24 hrs. One day after the formulations were reweighed and the moisture content % was calculated by the following equation (Ravichandiran and Manivannan, 2015).

$$\text{Percentage moisture content} = (\text{Weight}_{\text{initial}} - \text{Weight}_{\text{final}})/\text{Weight}_{\text{initial}} \times 100$$

2.3.3. Drug content

Drug content study performed, by dissolving about 1 cm × 1 cm film in 10 mL pH 7.4 phosphate buffer:methanol 3:1 (v/v) and the obtained solution filtered using membrane filter (0.45 μm).

Mupirocin concentration was measured at 221 nm. The test was repeated five times (Bavarsad et al., 2016).

2.3.4. HPLC analysis

For HPLC assay studies, HPLC equipment with a gradient pump, thermostable column department (t C18 column (5 μm, 150 × 4,6 mm)) and a UV detector supplied by Agilent 1100. The mobile phase consisted of methanol:water 80:20 (v/v). O-phosphoric acid adjust pH at 5. The flow rate was set to 1 mL/min and temperature of column was set at 25 ± 1 °C. The run time was 5 min and the optimum wavelength was 221 nm. The developed method was validated for precision, specificity, accuracy, selectivity and stability, recovery percentage of MPR (Amrutiya et al., 2009).

2.3.5. Swelling studies

To detect the swelling ability of formulations, 1 × 1 of films were chosen and then the films were placed in pH 7.4 PBS medium at 32 ± 1 °C. Films were removed from the medium after 5 min, 15 min, 30 min and every hour until 24 h. The water of film surface was taken with paper, and formulation was reweighed. The experiment was carried out five times. Percentage swelling was calculated.

Percentage swelling = (weight of swollen film after time − weight of 1 × 1 film at zerotime)/weight of insert at zerotime × 100

2.3.6. Uniformity of weight

Weight uniformity studies were done by weighting three different films of each batch. The uniform size at random and average weight was calculated (Nilani et al., 2011).

2.3.7. FT-IR spectroscopy of polymer films

FT-IR spectrophotometer was used so as to examine interactions between polymers and drug which can lead to different characteristics. Formulations were placed on an ATR crystal and maximum pressure was applied by using a pressure clamp to allow for intimate contact of the films with the ATR crystal. The spectra study region was from 4000 to 400 cm^{-1} while are baseline corrected and converted to the absorbance mode (Pawar et al., 2013; Siafaka et al., 2016d).

2.3.8. Morphology of the films

Scanning electron microscopy (SEM; Zeiss Evo HD 15, Germany) was used for evaluated the surface morphology of all formulations at 12 kV. Small pieces of formulations were cut into and mounted on 15 mm stubs with double sided adhesive carbon tape. The photos of the formulations were obtained with a magnification of 5000× (Boateng et al., 2013).

2.3.9. Tensile strength

Tensile strength of the formulations was studied using a Texture Analyzer (TA. XTPlus, Stable Micro Systems, UK). A film formulation (2 × 2 cm dimensions) was held between 2 clamps and pulled by the top clamp at 0.5 mm/s rate. The force and elongation were detected when the film broke off. Each formulation was performed in triplicate. The tensile strength and elongation at break were determined (Sezer et al., 2007).

2.3.10. Stability

Stability studies were performed for F6, F7 and F8 as per the International Conference on Harmonization guidelines. MUP-loaded films were kept at 4 ± 1 °C in the refrigerator and 25 ± 2 °C (relative humidity 60%) and 40 ± 2 °C (relative humidity 75%) for 6 months in the stability cabinets. MUP content, physical appearance and sterility were evaluated for films. The experiments were repeated three times (Üstündağ-Okur et al., 2015).

2.3.11. In vitro drug release studies

A dissolution apparatus (Pharmatest PTWS 820D) was used so as to study *invitro* release. The paddle method (USP II) was also applied. Conditions were the following: 60 rpm, temperature = 32 °C, dissolution time: 48 h. 500 mL of pH 7.4 phosphate-buffered saline was used as the release medium. At specific time points, 1 mL of samples were taken, and immediately after each sampling, the same volume of fresh buffer was added to the incubation medium. Mupirocin amount was analyzed by HPLC as it is described in 2.4.1 (Aoyagi et al., 2007).

2.4. Microbiological studies of films

Antibacterial activity of films was detected by well agar diffusion technique according to Clinical and Laboratory Standards Institute guidelines. Various bacteria strains such as *Escherichia coli* (ATCC 8739), Enterococcus hirae (ATCC 10541), *Staphylococcus aureus* (ATCC 6538), *Pseudomonas aeruginosa* (ATCC 27853), Bacillus cereus (ATCC 7064), Klebsiella pneumoniae were applied and inhibition zones were measured after formulation use. The strains were incubated for 18 h at nutrient agar at body temperature. Active cultures were aseptically suspended in sterile saline solution (0.85% w/v) and were adjusted to give an inoculum with an equivalent cell density to 0.5 McFarland. About 100 μL of each bacterial suspension were separated evenly onto Mueller-Hinton II agar by sterile spatule and dried. 10 mm plates were filled with 100 μL of formulations. For Mupirocin and Chitosan, sterile discs were placed onto agar plates and 20 μL of each commercial solution was applied to the discs. Plates were incubated at 37 ± 0.5 °C for 24–48 h and the zones of inhibition were measured. Each test was performed in triplicate and the zone inhibition was determined. The experimental groups were Mupirocin; Chitosan, F6MUP; F6, F7MUP; F7, F8MUP; F8 and commercial solution.

2.5. Ex vivo bioadhesion studies

The bioadhesion study was evaluated by texture at 37 °C. Mice abdominal skin was used for *ex vivo* bioadhesion work. The skin was fitted on the equipment, and 100 μL water was dropped on the skin before the measurement. The formulation was cut and fitted to the P/10 cylindrical probe (Lucite, UK). The probe was lowered onto the skin with a fixed speed (1 mm/s^{-1}) and 1 N contact force was applied. After 30 s contacting, the probe was then moved upwards at 1 mm/s^{-1}. Work of adhesion (mJ/cm^2) and peak detachment force (N/cm^2) were calculated from force-distance plot using the Texture Exponent program. Each measurement was done in triplicate (Sezer et al., 2007).

2.6. Ex vivo permeation studies

Ex vivo permeation studies were performed for F6, F7, and F8 film formulations containing 2% mupirocin using vertical Franz diffusion cell. pH 7.4 phosphate buffer was used as receptor medium, and the temperature were maintained at 37 ± 1 °C. Sink conditions were maintained during *ex-vivo* permeation studies. Full thickness Balb/c mice abdominal skin was used for the studies; the outer skin surface hair was removed, and the skin was carefully dissected and rinsed with saline. The suitable size of the film or certain amount of film with same mupirocin content was mounted on the mice skin. The receptor fluid was periodically withdrawn at suitable time intervals from the sampling arm of receptor chamber and was replaced with fresh buffer. Aliquots of the collected sample were analyzed for their mupirocin content (Bavarsad et al., 2016).

2.7. In vivo studies

2.7.1. Experimental animals

In vivo experiments were performed and prior to these studies ethical approval was acquired from the Istanbul Medipol University Ethical Council (No: 25.01.2018-02). The balb-c mice (26–30 g) were fed ad libitum water and food under laboratory conditions and kept in standard cages (23 ± 2 °C and 12 h/12 h dark-light cycle). The European Community guidelines as accepted principles for the use of experimental animals, were adhered to.

2.7.2. Experimental groups and excisional wound model

Twenty-four mice were divided into 4 groups and named, as follows:

Group 1: Untreated (UG) as the control group.
Group 2: Blank film (FG) group (F6 film).
Group 3: Mupirocin film (MG) group (F6MUP film).

Group 4: Bactroban® cream (GlaxoSmithKline, Turkey) (BG) as the standard group.

The mice were anesthetized with xylazine (80 mg/kg) and ketamine (10 mg/kg) and the back of each animal was depilated and washed with solution of povidone-iodine. The two excisional wounds (5 mm diameter per lesson) were created on the shaved area by the punch biopsy. The standard drug and the formulations were topically applied one a day for 10 days (Okur et al., 2018).

2.7.3. Wound area measurement

In order to evaluate contraction of wound, photographs were taken at days 0, 2, 4, 6, 8, and 10 by a digital camera (Canon, Japan), using 90° angle to the plane of the injury. Camera lens poses vertically to wounds. Wound areas were computed by an image analysis program (Image J., NIH, USA) (Okur et al., 2018). The healing effect of formulations was calculated by the following formula: % Wound contraction = (Actual Wound Area/Total Wound Area) × 100.

2.7.4. Histopathology examination

The wound area was cutted from fat. The skins were wiped off and fixed in 10% solution of formalin for 24 h; after-ward washed, dehydrated with ethanol, immersed in xylene and were lastly embedded in paraffin wax at 56 °C. 5 μm paraffin blocks were cut by using microtome. Sections were painted with Hematoxylene & Eosine and evaluated with the light microscope (Nikon). Wound healing activity was appraised via use of the scoring system. Briefly the scoring was maintained as score 1 for poor epidermal organization in ≥60% of the tissue, score 2 for incomplete epidermal organization in ≥40% of the tissue, score 3 for moderate epithelial proliferation in ≥60% of the tissue and score 4 for complete epidermal remodeling in ≥80% of the tissue. Scoring was recorded as 1 for thin granulation layer, 2 for moderate granulation layer, 3 for thick granulation layer, 4 for very thick granulation layer for thickness of the granulation tissue. For angiogenesis, only ripe vessels were considered and determined by the existence of erythrocytes. In order to differentiate well formed capillaries from poorly formed ones, the existence or lack of edema, thrombosis, hemorrhage, congestion, and intravascular or intervascular fibrin formation were all evaluated, as score 1 describes changed angiogenesis (one to two vessels/site) characterized by a high degree of edema, presence of hemorrhage, occasional congestion and thrombosis; score 2 describes few newly formed capillary vessels (3–4/site), moderate edema and hemorrhage, occasional congestion, intravascular fibrin deposition and absence of thrombosis; score 3 describes newly formed capillary vessels (5–6/site) and score 4 describes freshly created and normal seeming capillary vessels (>7/site) (Ayla et al., 2017).

2.7.5. Statistical analysis

All statistical analyses were evaluated with GraphPad Prism 7.0 program. Outcomes were given as means ± standard error of the mean. Statistical significance between groups was analyzed by one-way ANOVA followed by Dunnett's post hoc test. Values for $p < 0.05$ were considered statistically significant.

3. Results and discussion

In Table 1 a list of the materials that were used in the present work, together with their abbreviations is provided. In the rest of the manuscript we will refer to the samples, where needed, by their abbreviations.

3.1. Preparation and characterization of film formulation

Solvent casting method is widely used in pharmaceutical technology field since the prepared films could possess interesting properties, such as increased drug dissolution when hydrophobic molecules are used (Siafaka et al., 2015a; Üstündağ Okur et al., 2018) alongside improved swelling ability and water sorption especially in case of hydrophilic polymers. When wound healing is studied, films with significant swellability can induce the healing process (Jin et al., 2016). In this research, the developed films were evaluated for their thickness, weight uniformity, moisture loss, MUP content. FT-IR spectroscopy was applied so as to study interactions between the components and MUP whereas SEM observation was carried out to check if the composite films present morphology that could affect their properties.

3.1.1. FT-IR spectroscopy and SEM analysis

Fig. 1 demonstrates SEM analysis of the composite films. It should be reported, that solvent casting method is unlikely to produce interesting architectonical structures (Ghosal et al., 2018) compared to other methods as electrospinning (Siafaka et al., 2016a,b,c,d) or phase separation (Siafaka et al., 2016a,b,c,d). In further, when polymer are blended so as to prepare film carriers, SEM analysis can provide useful information about their miscibility. In this study, F1 and F2 revealed non porous surface. The smooth morphology of F1 and F2 films is typical of chitosan films. It has been reported that neat chitosan films lack apparent pores (Casariego et al., 2009; López-Mata et al., 2015); nonetheless, a research documented the presence of pores uniformly distributed on the film surface (Pereda et al., 2011). It is documented that the specific morphology depends on the nature of the chitosan (acetylation degree and molecular weight). In further, the addition of plasticizers such as PEG and PPG also reduces the number of structural disruptions such as cracks and pores (Maria et al., 2016). F3 film which composed of sodium alginate showed a structure of interconnected spherical particles which also indicates phase separation. F4 and F5 depicted a leaf-like morphology which is typical when phase separation occurred (Siafaka et al., 2016d). At these films, the separation is between chitosan and sodium aginate. F6 presents homogenous and smooth surface with spherical particles indicating the miscibility of the chitosan and carbopol (Singh et al., 2017a,b). F7, F8 and F9 did not have an interesting surface appearance since they show a homogeneous surface without phase separation between chitosan and carbopol, indicative of a good interaction between the components (Lozano-Navarro et al., 2018). Finally, F10 and F11 depict an agglomerated surface after solvent evaporation with cracks and pores (Singh et al., 2013).

Table 1
Formulation codes of polymer composite films.

Ingredients (% w/v)	F1	F2	F3	F4	F5	F6	F7	F8	F9	F10	F11
Chitosan	1	1	–	1	1	1	1	1	1	–	–
Sodium alginate	–		1	1	1	–	–	–	–	1	1
Carbopol	–	–	–	–	–	0.5	0.5	0.5	0.5	0.5	0.5
Glycerine	–	–	–	5	–	5	–	–	10	5	–
PEG 400	5	–	–	–	–	–	5	–	–	–	–
Propylene Glycol	–	5	5	–	5	–	–	5	–	–	5
Mupirocin	2 F1MUP	2 F2MUP	2 F3MUP	2 F4MUP	2 F5MUP	2 F6MUP	2 F7MUP	2 F8MUP	2 F9MUP	2 F10MUP	2 F11MUP

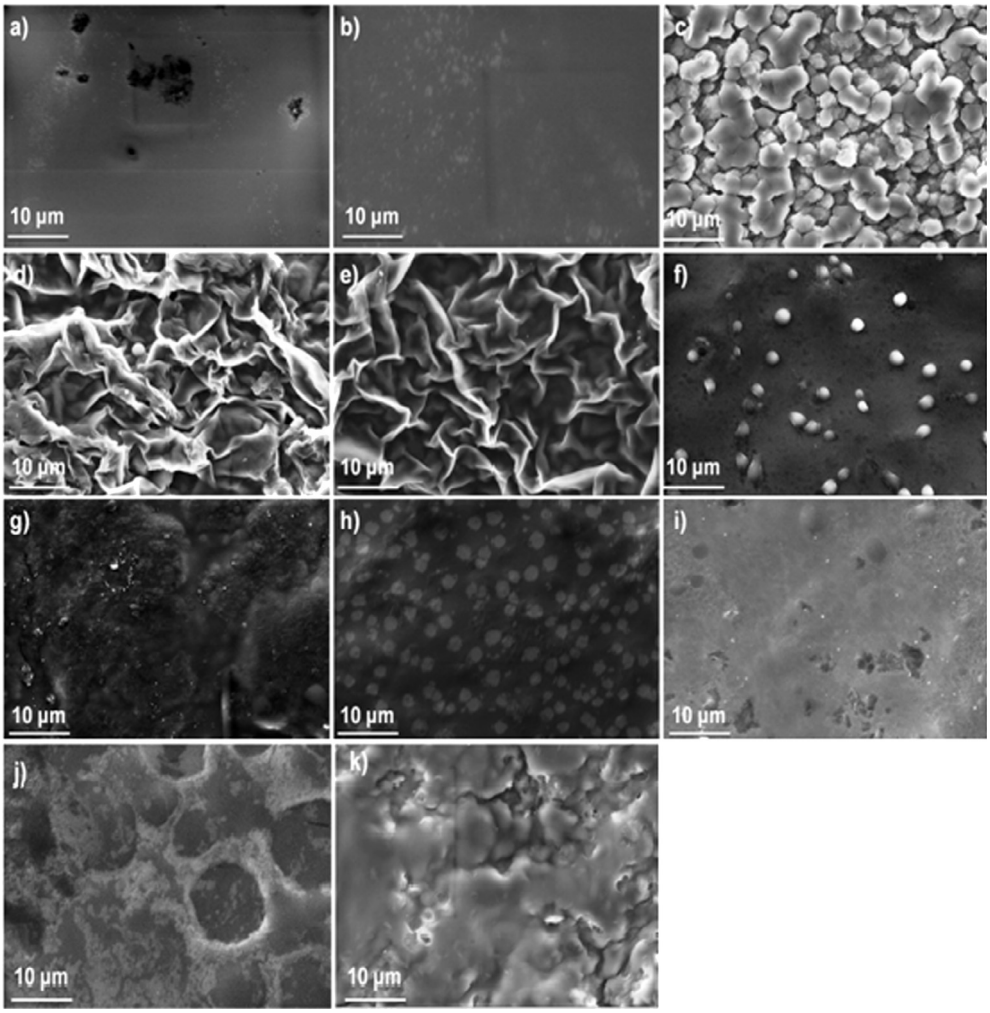

Fig. 1. SEM images of the films (a) F1, (b) F2, (c) F3, (d) F4, (e) F5, (f) F6, (g) F7, (h) F8, (i) F9, (j) F10 and (k) F11.

Figs. 2–5 exhibit FT-IR spectra of the prepared composite films. Fig. 2 depicts the spectra of F1 and F2 films neat and with MUP. In case of neat chitosan, the characteristic absorption bands at 1659 (amide I), 1582 (—NH_2 bending) and 1381 cm^{-1} (—CH_2 bending) are observed. The broad band at 3422 $cm^{-1}$is assigned to the hydroxyl group (Bhattarai et al., 2006; Filippousi et al., 2015; Kyzas et al., 2014; Siafaka et al., 2015a; Siafaka et al., 2016d). The two peaks at 902 and 1157 cm^{-1} are resulted from the saccharide structure of chitosan. The strong absorptions of PEG400 are assigned to —CH_2CH_2- stretching around 2874 and 3440 cm^{-1} demonstrating the presence of saturated carbons (CH_2CH_2) n. Mupirocin FT-IR exhibits the characteristic carbonyl group at 1720 cm^{-1} and 1657 corresponds to C=C whereas at 3480 and 3278 cm^{-1} found the stretching of OH while —CH_2CH_2– stretching is observed at 2929–2862 cm^{-1}. F1 spectrum indicates the presence of each component. The broad band at 3381 cm^{-1} is due to the hydroxyl group, at 1659 cm^{-1} corresponds to lactic acid which used for the dissolution of chitosan. Interactions between chitosan and PEG have not been seen given that F1 spectrum is similar to that of CS spectrum. In case of MUP loaded F1, although, each used polymer presents functional groups such as NH_2 or COOH which can interact with the OH or COOH groups of Mupirocin drug, such interactions haven't been identified. This fact can be ruled out given that new bands or shifting in lower wavenumbers was not

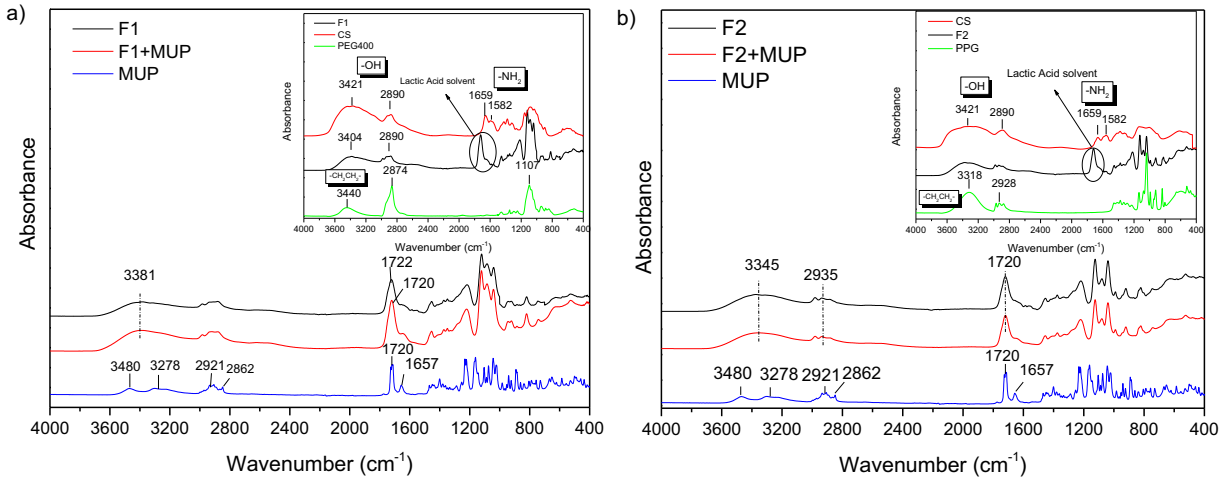

Fig. 2. FT-IR spectrum of (a) F1 formulation loaded with MUP. Inset: CS, PEG and F1 unloaded materials and (b) F2 formulation loaded with MUP. Inset: CS, PPG and F2 unloaded materials.

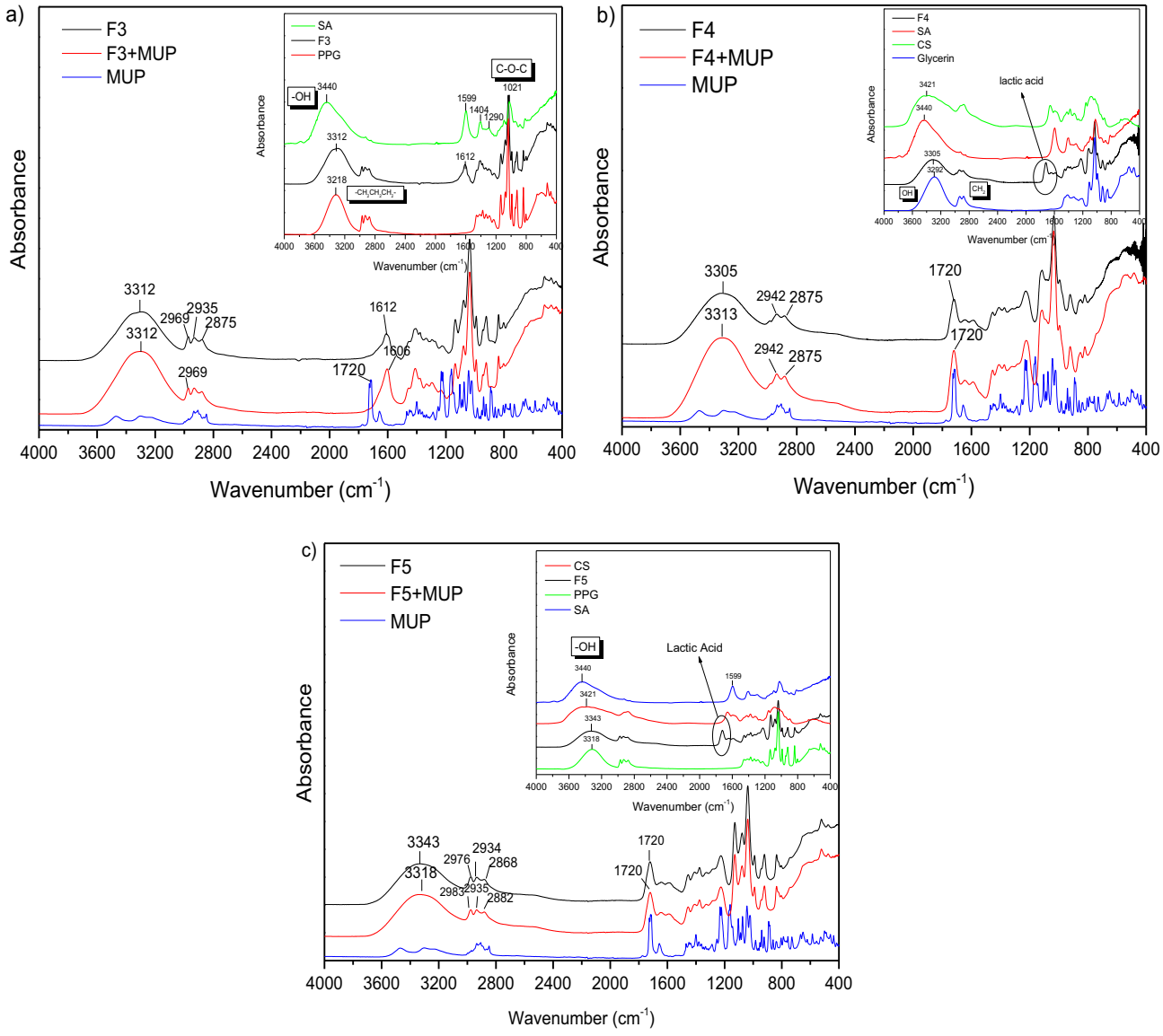

Fig. 3. FT-IR spectrum of (a) F3 formulation loaded with MUP. Inset: SA, PPG and F3 unloaded materials, (b) F4 formulation loaded with MUP. Inset: CS, SA, Gly and F4 unloaded materials and (c) F5 formulation loaded with MUP. Inset: CS, SA, PPG and F5 unloaded materials.

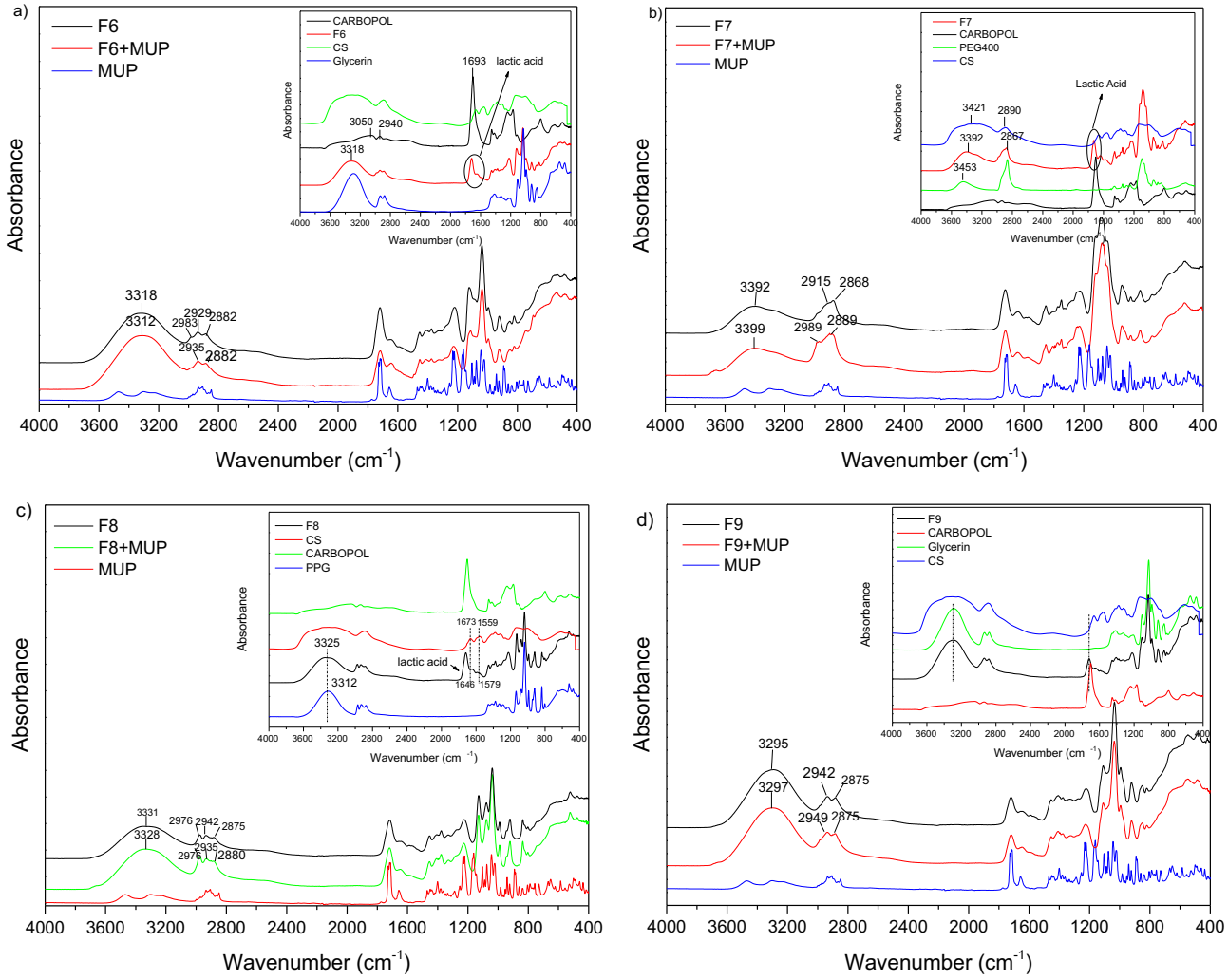

Fig. 4. FT-IR spectrum of (a) F6 formulation loaded with MUP. Inset: CS, Carbopol, Gly and F6 unloaded materials, (b) F7 formulation loaded with MUP. Inset: CS, Carbopol, PEG400 and F7 unloaded materials, (c) F8 formulation loaded with MUP. Inset: CS, Carbopol, PPG and F5 unloaded materials and (d) F9 formulation loaded with MUP. Inset: CS, Carbopol, Gly and F9 unloaded materials.

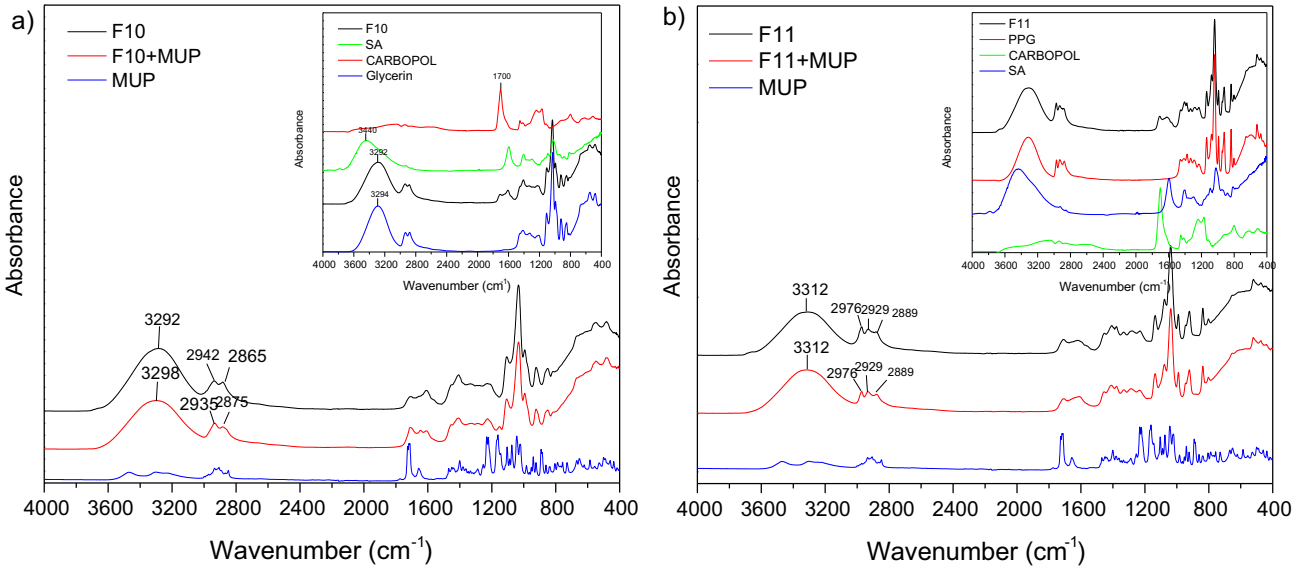

Fig. 5. FT-IR spectrum of (a) F10 formulation loaded with MUP. Inset: Carbopol, SA, Gly and F10 unloaded materials and (b) F11 formulation loaded with MUP. Inset: Carbopol, SA, PPG and F11 unloaded materials.

observed (Siafaka et al., 2016d). This factor is important for the stability of the formulations.

In case of F2 formulation, where PPG was used instead of PEG 400 we had a similar spectra for loaded and unloaded materials. It should be noted that PPG spectrum present a broad band at 3318 cm^{-1} which is attributed to the OH stretch of the PPG end group, the C—O stretching vibrations are seen near 1090 cm^{-1} whereas CH_3 stretching and deformation vibrations near 2890 and 1380 cm^{-1} (Schmidt et al., 2009). It can be said that F2 spectrum follows PPG spectra considering that PPG is in higher concentration in the film. In addition, bands corresponding to the drug was not observed or newer vibrations indicating the stability of the product.

Fig. 3 shows the spectrum of sodium alginate and its characteristic peaks. It can be observed that the absorption bands around 1610 cm^{-1}, 1416 cm^{-1}, and 1306 cm^{-1} are attributed to stretching vibrations of asymmetric and symmetric bands of carboxylate anions, respectively. Further, mannuronic acid functional group is seen at 884 cm^{-1} and the uronic acid at 939 cm^{-1}, OH functional group at 3440 cm^{-1}, and CH_2 stretching at wavenumber 2928 cm^{-1}. The bands around 1030 cm^{-1} (C—O—C stretching) presenting in the IR spectrum of sodium alginate are attributed to its saccharide structure. In addition, the bands at 1617 and 1417 cm^{-1} are assigned to asymmetric and symmetric stretching peaks of carboxylate salt groups (Li et al., 2008). It can be concluded that F3 films present also the bands of SA and PPG. However, new bands corresponding to new products were not obtained. In addition, interactions (mostly hydrogen bonding) between PPG and SA can easily concluded since the adsorption band of OH group was shifted in lower wavenumbers than SA and higher than PPG. Glycerin spectrum exhibit bands at 3300 cm^{-1} is due to OH stretching modes whereas the peaks around 2900 cm^{-1} are due to the CH stretching modes. The peaks between 1500 and 700 cm^{-1} are due to CH bending (1500–1200 cm^{-1}) and C—O stretching (1200–900 cm^{-1}). In case of F4, it can be said that after the addition of the complex plasticizer of Glycerin the absorption band of "—OH" shifted to a lower wavenumber, showing that hydrogen bonding is taking place between the hydroxyl group of GLY and other ingredients showing that Glycerin have a plasticizing effect for PVA (Puyou et al., 2014). Moreover, when MUP loaded to F4 film a shifting in higher wavenumbers for OH band is observed, revealing also interactions. F5 formulation comprised from chitosan, sodium alginate and polypropylene glycol. F5 spectrum presents the OH band at 3343 cm^{-1}, three band between 2950 and 2850 cm^{-1} region which corresponds to PPG addition whereas at 1720 cm^{-1} band is associated to lactic acid solvent. It can be concluded that F5 formulation follows mostly PPG spectrum however the shifting in higher wavenumber of the OH band can indicate interaction between the components. After MUP addition, OH is altered in lower wavenumbers which can reveal that MUP interact with the component.

Fig. 4 exhibits spectra of neat F6, F7, F8 and F9 and loaded with MUP. These formulations are composed by CS and Carbopol as main ingredients. Carbopol is a water soluble polymer used as used as an emulsifying, stabilizing, suspending, thickening and gelling agent. Carbopol spectrum presents a broad band at3500 and 2940 cm^{-1} (due to OH and N—H stretching vibrations), a sharp peak at 1693 cm^{-1} (due to asymmetric —COOH stretching) at 1544.0 cm^{-1} (due to symmetric —COOH stretching of carbopol). In further, an absorption band at 1170.3 cm^{-1} (due to C—O—C stretching in carbopol), 1451 cm^{-1} (due to C—O stretching and O—H in plane bending for acrylates), at about 1243 cm^{-1} (due to C—O—C asymmetric stretching for acrylates) (Singh et al., 2013).

It can be said that F6 spectrum follows glycerin spectrum due to the plasticizing effect. When MUP was added similar spectrum was seen which cannot conclude interactions between drug and polymers. F7 and F8 don't have GLY but PEG400 and PPG, respectively. Thus, F7 shows similar spectrum with PEG400 and F8 with PPG. In case of F7, OH band (3392 cm^{-1}) is shifted to lower wavenumbers than PEG (3453) revealing that interactions between components can be found (hydrogen bonding). However, MUP addition did not alter the spectrum dramatically and it is believed that MUP did not affect the film. In similar way were the results for F8 films. F9 also comprised from CS, GLY and Carbopol. It can be said that F9 spectrum follows GLY spectrum and strong interactions have not been identified.

Fig. 5 exhibits spectra of neat F10 and F11 and loaded with MUP. The above formulations comprised from SA and Carbopol as main ingredients. F10 which embedded GLY mainly has similar spectrum with GLY but SA bands appeared also between 1700 and 1500 cm^{-1}. However, it should be noted that when MUP was added the OH band shifted to higher wavenumbers. F11 presents the bands of PPG and SA demonstrating that all components interact with each other. Nonetheless, MUP addition did not alter spectrum.

To conclude, from FT-IR spectroscopy studies, it can be said that strong interactions between mupirocin and the other ingredients within the formulation did not depict, thus the formulations present strong stability during their shelf life.

3.1.2. Thickness, swelling ability and mechanical strength studies

When potential wound dressings are evaluated, several parameters such as thickness, swelling ability, tensile strength and elongation should be studied so as to check their suitability as drug delivery systems and healing promoters. Herein, thickness tests measured by a micrometer showed that films thickness ranged from 0.26 to 0.841 mm. F7 film (chitosan 1%, carbopol 0,5%, PEG 400 5%) with 0.26 + 0.02 mm is the thinnest film and the F2 film (chitosan 1%, propylene glycol 5%) with 0.841 + 0.026 was the thickest film. Thickness is acceptable and thus all films can be applied as wound dressings. Weight of films ranged from 0.029 to 0.078 mg whereas drug content was found relatively high as it was expected since solvent casting leads to high drug loading. Accordingly, tensile strength and elongation was tested in this work in order to evaluate the strength and elasticity of the composite films.

It has been reported that the ideal wound dressings should be elastic, so as to follow skin movements and possesses adequate resistance to mechanical abrasion (Mohamad et al., 2014). Chitosan films are less flexible and possess poor mechanical properties, especially in terms of their inferior ability to elongate (Prateepchanachai et al., 2017). Both chitosan and sodium alginate films become brittle after solvent casting (Ma et al., 2017). Therefore, the use of plasticizers for CS or SA film formation is very important. Plasticizers are generally nonvolatile, high boiling, low molecular weight compounds which when added to a polymer matrix improve its processability, flexibility, and stretch ability by modifying the mechanical properties making the films more ductile. By adding plasticizer to a polymeric material, elongation at break, toughness and flexibility are expected to increase, on the other hand tensile stress, hardness, electrostatic chargeability, Young's modulus and glass transition temperature are expected to decrease (Gal and Nussinovitch, 2009; Rahman and Brazel, 2004). The commonly used plasticizers in dermal delivery patches include phthalate esters, phosphate esters, fatty acid esters and glycol derivatives (Gngr et al., 2012; Lim and Hoag, 2013). In this work, we chose polyethylene glycol (PEG), propylene glycol (PPG), and glycerin (GLY) so as to improve the mechanical properties of the prepared films.

The mechanical properties are shown in Table 2. It can be said that films that show higher tensile strength correspond to stronger film while the tensile strength of a film is the maximum stress that a film can withstand being stretched before necking or cracking. In

Table 2
Evaluation parameters of the composite films.

FC	Uniformity of weight (g)	Moisture loss (%)	Thickness (mm)	Drug content (%)	Tensile strength (N/cm^2)	Elongation at break (N)
F1	0.078 ± 0.005	0.753 ± 1.581	0.73 ± 0.018	87.521 ± 4.128	0.777 ± 0.067	142.107 ± 6.184
F2	0.076 ± 0.004	−0.494 ± 1.639	0.841 ± 0.026	94.099 ± 4.223	0.069 ± 0.012	242.292 ± 32.157
F3	0.033 ± 0.003	−50 ± 00000	0.309 ± 0.01	85.702 ± 1.910	2.799 ± 0.369	15.225 ± 2.369
F4	0.058 ± 0.003	8.6371 ± 1.083	0.471 ± 0.017	80.212 ± 7.269	1.531 ± 0.569	40.125 ± 2.439
F5	0.054 ± 0.002	−7.372 ± 0.277	0.477 ± 0.015	87.181 ± 1.247	0	0
F6	0.06 ± 0.0005	1.120 ± 2.067	0.504 ± 0.018	93.852 ± 3.473	0.695 ± 0.112	211.763 ± 27.119
F7	0.035 ± 0.006	6.291 ± 3.59	0.26 ± 0.019	61.537 ± 2.513	6.322 ± 3.057	120.158 ± 26.485
F8	0.046 ± 0.002	−11.575 ± 2.632	0.37 ± 0.018	73.982 ± 1.284	1.065 ± 0.351	150.045 ± 32.667
F9	0.081 ± 0.005	4.566 ± 1.537	0.722 ± 0.015	82.846 ± 1.712	0.035 ± 0.004	146.588 ± 2.777
F10	0.033 ± 0.002	15.313 ± 2.495	0.332 ± 0.015	80.755 ± 1.426	2.089 ± 0.092	107.787 ± 9.263
F11	0.029 ± 0.002	−40.518 ± 3.290	0.306 ± 0.012	85.705 ± 4.129	105.237 ± 9.721	21.592 ± 2.288

this work, the highest tensile strength was that of F11 film (105.237 ± 9.721 (N/cm^2)), followed by F7 > F3 > F10 > F4 > F8 > F1 > F6 > F2 > F9 > F5. Elongation at break was higher in case of F2 (242.292 ± 32.157 N) followed by F6 > F8 > F9 > F1 > F7 > F10 > F4 > F11 > F3 > F5.

Among the films containing chitosan and PEG or PPG as plasticizer (F1, F2), tensile strength was higher in case of PEG addition whereas elongation was greater in case of F2. In case of films containing CS, Carbopol and one of the plasticizer PEG, PPG or GLY, F7 had the highest tensile strength due to PEG addition, followed by F8(PPG), F6(GLY5) and F9(GLY-10). It can be ruled out that increasing GLY content tensile strength is decreased. Elongation was highest in case of F6 followed by F8 and F9 of which elongation is almost similar. F7 had the lowest elongation of the four films, which is rational as the tensile strength was greater. In case of F7 and F8, it can be reported that both of the films present improved tensile strength and elongation which it can be attributed to the addition of carbopol and PEG or PPG. Carbopol was applied so as to increase the mucoadhesion of the prepared films. However, some reports recommend that carbopol can play a role in the mechanical properties of a system (Peh and Wong, 1999).

F3 film contains sodium alginate and PPG as plasticizer. For this film, tensile strength is 2.799 ± 0.369 N/cm^2 whereas elongation is the lowest of all formulations. F10 and F11 present low and high tensile strength, respectively which can be attributed to the GLY and PPG addition.

From the above, F6 film seems to possess the ideal mechanical properties given that presents significant tensile strength and high elongation, properties which are ideal for dermal films.

Swelling ability is quite significant parameter when wound healing dressings studied. Carbohydrates such as chitosan (Siafaka et al., 2016c,d) and sodium alginate (Huang & Yang, 2009) are known to be swellable in physiological fluids. Similarly, Carbopol since composed of acrylates present swelling ability which however affected by erosion during time. Swelling ability is seen in Fig. 6a and b. F4 and F5 comprised from Chitosan and Sodium Alginate which both are high swellable polymers. F4 also has glycerine as plasticizer. Both films absorb water and swell with passage of the time. However, after 24 h a weight reduction is observed probably due to dissolution of sodium alginate in pH = 7.4. Carbopol is a component of F6-F9 films. Carbopol has hydroxyl groups which at high pH = 7.4 and 8.0 are converted to carboxylate anions with an expansion of the gel network due to electrostatic repulsion resulting in increased swelling. The ionization of carboxylic groups under basic conditions increases the hydrophilicity of the molecular chains also leads to the generation of negative charge repulsion among them, and hence, hydrogels show higher swelling ability. Interestingly, F6-F9 the first 20 min swelled and volume and weight increased. After this, weight is decreased due to carbopol aqueous solubility.

3.1.3. Stability

MUP-loaded films (F6, F7 and F8) were kept at 4 ± 1 °C in the refrigerator and 25 ± 2 °C (relative humidity 60%) and 40 ± 2 °C (relative humidity 75%) for 6 months in the stability cabinets according to the International Conference on Harmonization guidelines. The samples were analyzed at 1, 3, and 6 month. It was found that there are no changes in visual appearance and clarity after 6 month. For F6 formulation 93.8–98.4% of initial drug content of formulations was kept its stability for in 6 month at 4 ± 1 °C in the refrigerator and 25 ± 2 °C (relative humidity 60%). At 40 ± 2 °C all formulations drug contents is lower than 30% after 6 month. According to the stability studies F6 formulation can be stored at 4 and 25 °C.

3.2. In vitro drug release studies

Mupirocin is slightly soluble in aqueous medium as it was previously reported and thus improving its release properties is quite significant (Cern et al., 2014). When swellable hydrophilic polymers are applied as drug carriers the release mechanism is driven by several phenomena as the liquid penetration within the polymer network, the swelling of hydrated polymer, drug diffusion throughout swollen matrix as well as the possible erosion (Siafaka et al., 2016d). In addition to these factors, sometimes a hydrated viscous layer is developed around the polymer film which acts as barrier and provokes the water penetration from dissolving the drug molecules. Consequently, it is quite difficult to examine the release mechanism of swellable matrices as studied in this work.

Fig. 7 depicts in vitro release studies using phosphate buffered saline (Siafaka et al., 2016d). Firstly, it can be said that MUP presents an improved release rate since F4-F9formulations exhibit that MUP was released at least in 60–100%. In addition, a progressive release rate is shown in case of F4, F5, F7, F8films which also present a low burst effect. In case of F6 and F9 films it can be ruled out that both of these films release the drug after the first hour. F4, F5, F6 and F9 released the whole amount of MUP however F7 and F8 had a difficulty to dissolve the drug. In conclusion, it seems that F6 film starts to release the drug after 1.5 h. As swelling studies indicate, F6 film reaches the maximum swelling ratio at 1 h and afterwards F6 weight decreases due to carbopol hydrophilicity. We can conclude that F6 presents high release rate and it is promising as wound dressing since almost 2 h after being in the release medium, releases fully Mupirocin drug. All he others formulations, reach the maximum release after 12 h of study.

3.3. Microbiological studies

Mupirocin is a natural crotonic acid derivative extracted from Pseudomonas fluorescens. It has been reported that MUP inhibits

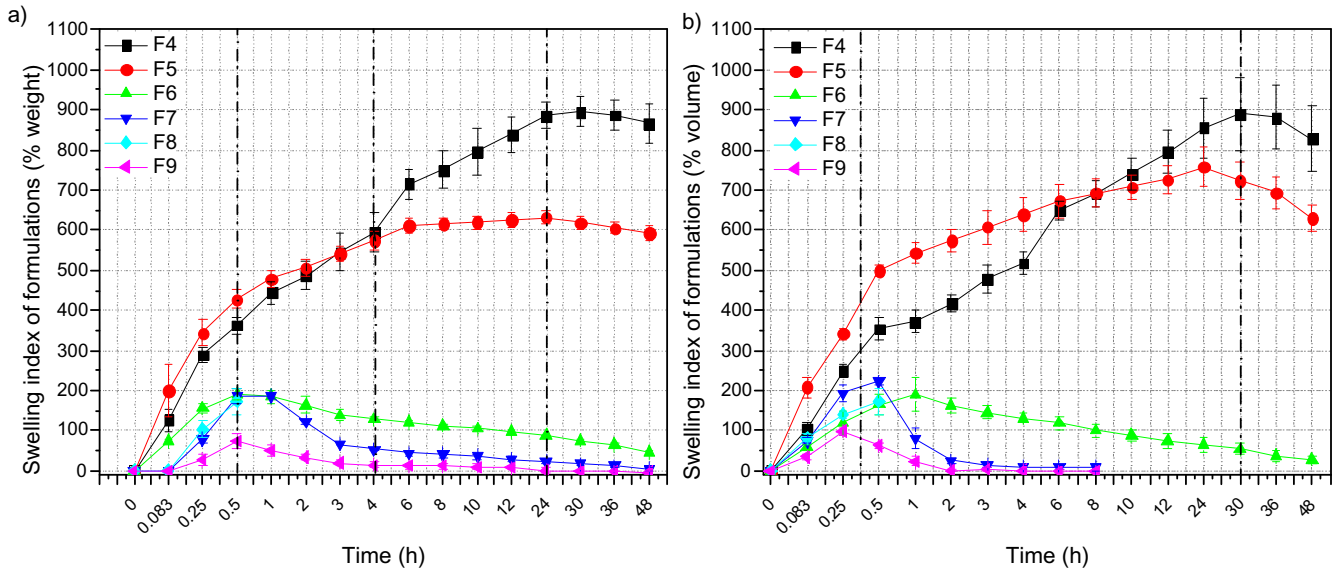

Fig. 6. (a) Swelling index of formulations (% weight) and (b) Swelling index of formulations (% volume).

bacterial protein synthesis by specific reversible binding to bacterial isoleucyl tRNA synthase. MUP also depicts excellent activity against gram-positive staphylococci and streptococci. Consequently, this antibiotic drug used for treatment of primary and secondary skin disorders, nasal infections, and wound healing. Herein, the antimicrobial activity of the composite films assessed against wound associated bacterial strains such as *Escherichia coli*, *Staphylococcus aureus*, *Pseudomonas aeruginosa*, Bacillus cereus, Enterococcus hirae, Klebsiella pneumoniae since the above strains have been isolated in several wound types (Dang et al., 2018; Khalid et al., 2017; Siafaka et al., 2016d).

Neat composite films and MUP loaded films present antibacterial property against the studied strains (Fig. 8). It could be concluded that dressings loaded with MUP showed advantageous activity against the strains compared to neat dressings. In particular, pure chitosan demonstrated activity against *E. coli*, *P. aeruginosa*, *S. aureus* while non inhibition was seen for *B. ceres*. NeatMUP, as it was expected presents high antibacterial ability against all strains. Almost similar antibacterial activity, express the neat composite films. When MUP was loaded into the film similar or higher antimicrobial activity was demonstrated compared to neat films. To conclude, the obtained results indicate that the MUP (F6-8) films possess antibacterial activity that could be used as wound dressing system so as to prevent wound colonization or severe infection. F6 film seems to be slightly superior compared to F7 and F8 film, and thus we can recommend it, as ideal wound drug delivery film.

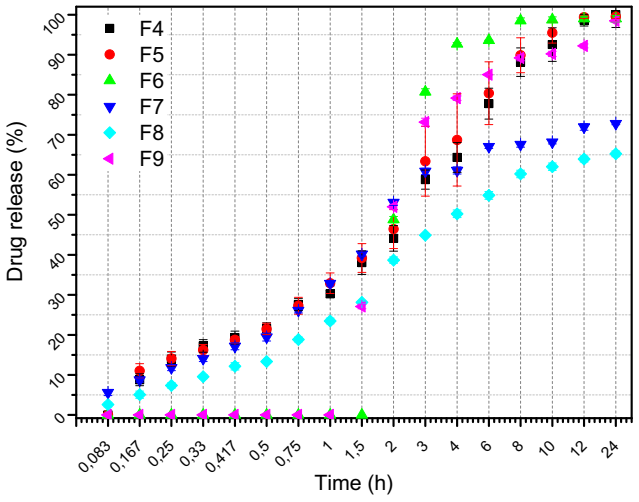

Fig. 7. *In vitro* drug release profile of formulations.

3.4. Ex vivo bioadhesion and permeation studies

Bioadhesion happens when two surfaces are contacted for an elongated time by interfacial energies (Tomczykowa et al., 2018). Bioadhesion is very important considering that if a dressing incorporates an adhesive that is too 'aggressive', then tissue damage may occur on its removal (Rippon et al., 2007). In addition to this, the bioadhesive features of the formulations used as topical drug carriers facilitate them to stick to the surface of skin, and then, extend the staying time (Tomczykowa et al., 2018). Table 3 showed *ex vivo* bioadhesion results of F6, F7 and F8 formulations. No significant difference in the bioadhesiveness of F6, F7 and F8 formulations were detected. Furthermore, *ex vivo* MUP permeation experiments using diffusion cells were performed to predict *in vivo* ability of MUP. In case of MUP permeation from F6, F7 and F8 films was determined after 12 h relatively low as 12.13 ± 0.95, 9.37 ± 0.92 and 4.10 ± 0.14%, respectively. According to the obtained data, the developed films can be applied safely as drug carriers for topical delivery of MUP. However, F6 formulation was chosen for *in vivo* studies since its physicochemical properties and the *ex vivo* bioadhesion and permeation results indicate its superiority against the other formulations.

3.5. In vivo studies

3.5.1. Macroscopic wound healing

Wound healing duration involves various phases such as granulation, collagenization, collagen maturation and scar maturation which are concurrent but independent to each other (Deshmukh et al., 2009). Representative photos of wound areas were taken on every 2 days during the treatment. The progressive wound healing samples of per group were shown in Fig. 9a. It was observed that treatments with blank film (FG) and mupirocin film (MG) formulations were not irritating to skin. In addition to this, on the

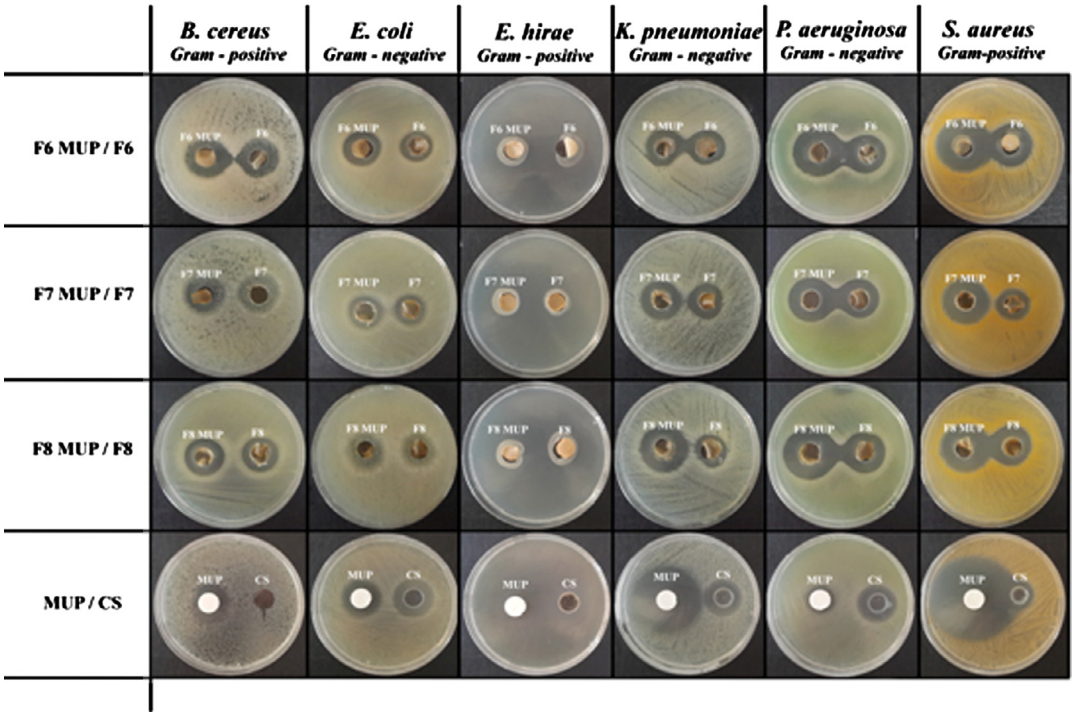

Fig. 8. Zone inhibition diameters of formulations against *S. aureus*, *E. coli*, *E. hirae*, *K. pneumoniae*, *P. aeruginosa* and *B. ceres*.

10th day, wound regions which were treated with bactroban cream (BG) and mupirocin film (MG) groups, were smooth and close to the normal skin color. In this work, F6 formulation was chosen for *in vivo* studies.

3.5.2. Wound contraction

Quantitative measurements of wound size are routinely used to assess initial wound size before and after debridement, as well as progress toward wound closure (Abu-Al-Basal, 2010). The wound sealing rates in animals were given in Fig. 9b. The % of wound area ranged from 86.41% to 21.36% in the period from in the period from 4 to 10 days in the control group. The % of wound area in mice treated with Bactroban (BG) ranged from 60.28 ± 2.27% (***) to 11.72 ± 1.27% (**) in the period from 4 to 10 days. The % of wound area in mice treated with Blank film (FG) ranged from 77.90.76% (**) to 11.821.44% (**) in the period from 4 to 10 days. The % of wound area in mice treated with Mupirocin film (MG) ranged from 51.01 ± 1.67% (***) to 5.88 ± 0.76% (***) in the period from 4 to 10 days. Mupirocin film formulation showed the highest decrease in % of wound area in comparison with control group. Although both groups contain MUP, the difference between MG and BG might be due to film formulations showed a long-acting effect than cream formulations. The objective of the injury therapy is to abbreviate the healing time or to decrease the unwanted results, the reupon scarring (Okur et al., 2018). In addition, FG showed remarkable effect as compared to control group. It can be considered that this effect is due to chitosan antimicrobial and haemostatic effects (Bano et al., 2017). The chitosan had a synergistic effect on the antibacterial properties, thus unloaded films also showed antimicrobial effects (Fig. 8). It is known that chitosan possess primary amino groups in their structures that play a major role in antibacterial activity. Moreover, chitosan can alter permeability characteristics of microbial cell membrane and further prevent the entry of materials or cause leakage of cell constituents that finally leads to death of bacteria (Üstündağ-Okur et al., 2015). The use of an antibiotic drug as a component in wound healing system is important so as to avoid wound infection. The antimicrobial agents can prophylactic act against infectious organisms and prevent incidents as sepsis.

Table 3
Ex vivo bioadhesion results of F6, F7 and F8 formulations.

FC	Work of bioadhesion mJ/cm^2	Bioadhesive force N/cm^2
F6	0.195 ± 0.020	0.432 ± 0.072
F7	0.121 ± 0.005	0.304 ± 0.057
F8	0.143 ± 0.002	0.305 ± 0.057

3.5.3. Histology of wound healing

The normal wound healing contains three successive but overlapping phases: hemostasis/inflammatory, proliferative, and remodeling phases (Wang et al., 2018). The proliferative phase of cutaneous wound healing, also called granulation phase, is characterized by reepithelization, angiogenesis, granulation tissue formation, and collagen deposition (Serra et al., 2017). It begins 3–4 days after damage and continues for 2–4 weeks (Greaves et al., 2013). In our work, angiogenesis, granulation tissue thickness, and epidermal dermal regeneration were examined separately.

Regular growth of granulation tissue during wound healing is one of the indicative of wound healing (Ayla et al., 2017). It was determined that MG (***) and BG (*) showed a significant granulation tissue thickness as compared to control, in accordance with the tissue samples. Moreover, it could be determined that thicker granulation tissue was occured in MG as compared to BG after treatment (Figs. 10 and 11). Angiogenesis, which is integral to successful wound repair, involves sprouting of wound-edge capillaries followed by their invasion into the site of damage (Shaw and Martin, 2009). Angiogenesis is triggered from the moment the haemostatic plug has formed as platelets release TGF-b, PDGF and FGF (Singh et al., 2017b). In this study, considering the results of histological evaluation, more blood vessel formation was detected on MG (***) and BG (*) as compared to control group (Figs. 10 and 11).

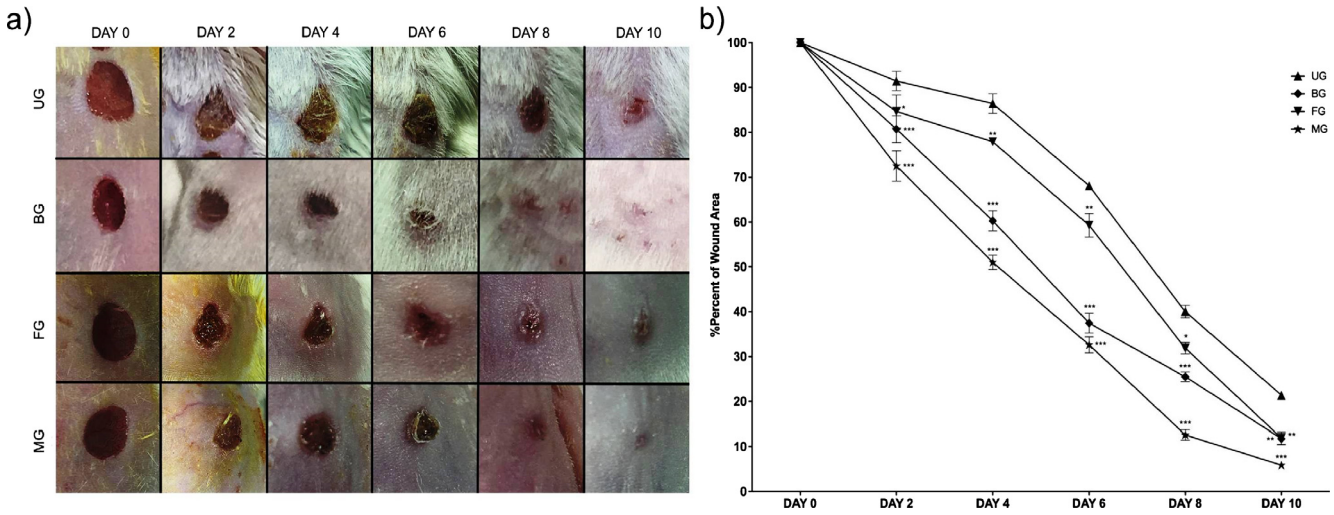

Fig. 9. (a) Macroscopic examples of Untreated (UG), Bactroban (BG), Blank film (FG), Mupirocin film (MG) groups at days 0, 2, 4, 6, 8, and 10. (b) Healing percentage of seam area in each group (Untreated (UG), Bactroban (BG), Blank film (FG), Mupirocin film (MG) groups).

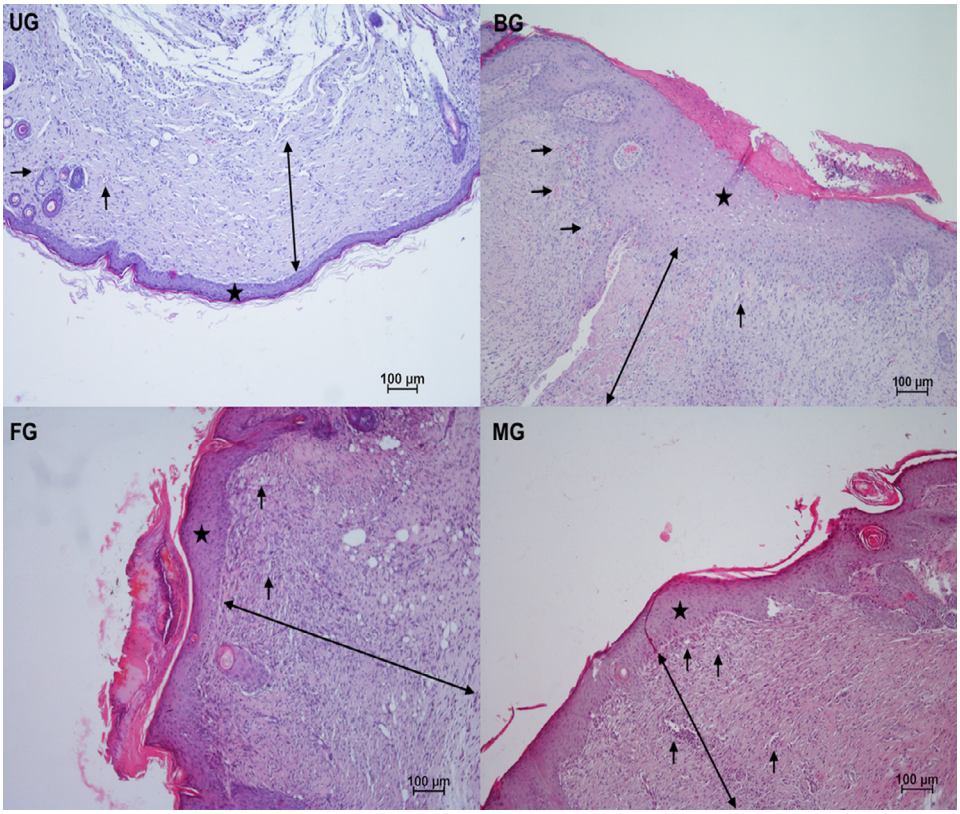

Fig. 10. Histopathologically observation of injured skin samples of the untreated (UG), bactroban (BG), blank film (FG), mupirocin film (MG) groups on 10th day (Hemotoxylen and eosin (magnification ×10). The scale bars represent 100 µm for figure. ★: Epidermal regeneration, →: Angiogenesis, blood vessels, ↔: Granulation formation.

Epidermal and dermal regeneration increment is a principal apprehension for the wound treatments (Basu et al., 2017; Okur et al., 2018; Zhang et al., 2018). This work also displayed that there was significantly higher % regeneration with the MG (**) and BG (*) compared to control (Figs. 10 and 11). It can suggested that mupirocin film group expedites the epidermal layer regeneration. Finally, it was determined that the mupirocin film group is more effective, compared to the market product group, to critical factors for wound healing such as epithelialization, granulation tissue thickness and angiogenesis.

4. Conclusion

The obtained data demonstrate the use of polysaccharides and other polymers in the development of novel dressings that could

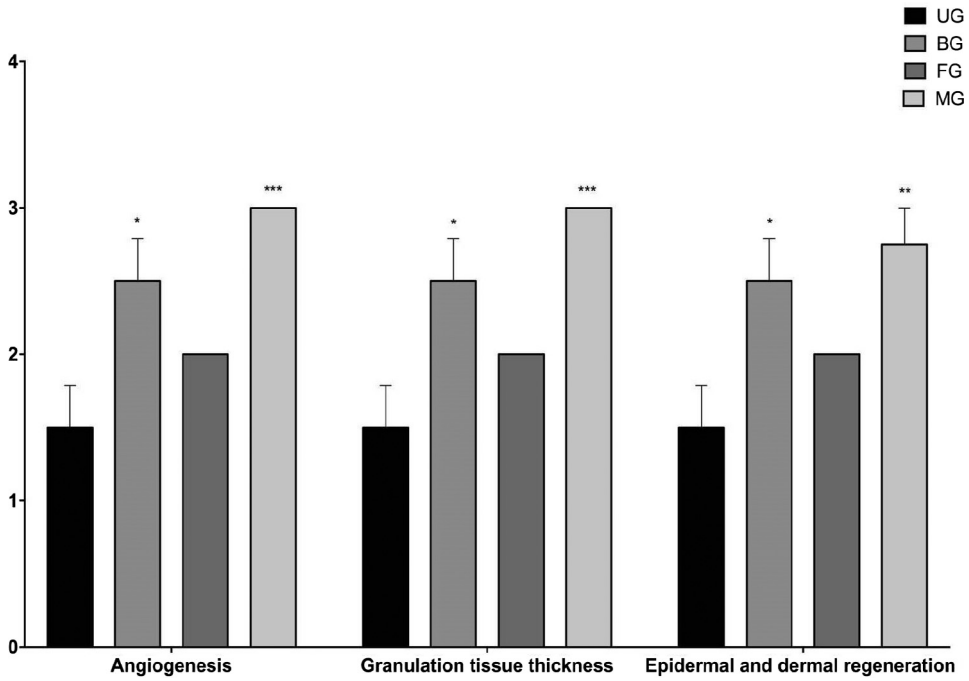

Fig. 11. Histological scores of granulation tissue thickness, angiogenesis and epidermal-dermal regeneration of untreated (UG), bactroban (BG), blank film (FG), mupirocin film (MG) groups.

afford significant clinical potential in would healing field. FTIR data showed that strong interactions between mupirocin and polymer matrices have not been depicted which ensure stability of the film during time. In further, morphology of the films was similar to other previously reported solvent casting films whereas thickness and weight were found as uniform. Swelling ability was improved but by the passage of the time swelling was decreased probably due to erosion or other mechanism. *In vitro* drug release studies demonstrated that MUP release was increased and in most case the drug was dissolved in high percentages. *Ex vivo* bioadhesion supports that F6 is the most bioadhesive formulation. *Ex vivo* permeation studies exhibit that a very low amount of mupirocin could cross the epidermis layer and thus the film can be safely applied for topical delivery. From *in vivo* studies, it can be concluded that the chosen due to its physicochemical characteristics, mupirocin film (F6) accelerates the regeneration of the epidermal layer while the film is more advantageous on epithelialization, granulation tissue thickness and angiogenesis compared to the commercial product.

Declaration of interest

The authors declare no conflict of interest.

Acknowledgements

The authors wish to thank the Pharmactive Drug Company, Istanbul, Turkey.

References

Abu-Al-Basal, M.A., 2010. Healing potential of *Rosmarinus officinalis* L. on full-thickness excision cutaneous wounds in alloxan-induced-diabetic BALB/c mice. J. Ethnopharmacol. 131, 443–450. https://doi.org/10.1016/j.jep.2010.07.007.

Alsarra, I.A., 2009. Chitosan topical gel formulation in the management of burn wounds. Int. J. Biol. Macromol. 45, 16–21. https://doi.org/10.1016/j.ijbiomac.2009.03.010.

Amrutiya, N., Bajaj, A., Madan, M., 2009. Development of microsponges for topical delivery of Mupirocin. AAPS PharmSciTech 10, 402–409. https://doi.org/10.1208/s12249-009-9220-7.

Aoyagi, S., Onishi, H., Machida, Y., 2007. Novel chitosan wound dressing loaded with minocycline for the treatment of severe burn wounds. Int. J. Pharm. 330, 138–145. https://doi.org/10.1016/j.ijpharm.2006.09.016.

Ayla, Ş., Günal, M.Y., Sayın-Şakul, A.A., Biçeroğlu, Ö., Özdemir, E.M., Okur, M.E., Ç içek-Polat, D., Üstündağ-Okur, N., Bilgiç, B.E., 2017. Effects of *Prunus spinosa* L. fruits on experimental wound healing. Medeni. Med. J. 32, 152–158. https://doi.org/10.5222/MMJ.2017.152.

Bano, I., Arshad, M., Yasin, T., Ghauri, M.A., Younus, M., 2017. Chitosan: a potential biopolymer for wound management. Int. J. Biol. Macromol. 102, 380–383. https://doi.org/10.1016/j.ijbiomac.2017.04.047.

Basu, A., Lindh, J., Ålander, E., Strømme, M., Ferraz, N., 2017. On the use of ion-crosslinked nanocellulose hydrogels for wound healing solutions: physicochemical properties and application-oriented biocompatibility studies. Carbohydr. Polym. 174, 299–308. https://doi.org/10.1016/j.carbpol.2017.06.073.

Bavarsad, N., Kouchak, M., Mohamadipour, P., Sadeghi-Nejad, B., 2016. Preparation and physicochemical characterization of topical chitosan-based film containing griseofulvin-loaded liposomes. J. Adv. Pharm. Technol. Res. 7, 91. https://doi.org/10.4103/2231-4040.184591.

Bhattarai, N., Ramay, H.R., Chou, S.H., Zhang, M., 2006. Chitosan and lactic acid-grafted chitosan nanoparticles as carriers for prolonged drug delivery. Int. J. Nanomed. 1, 181–187. https://doi.org/10.2147/nano.2006.1.2.181.

Boateng, J.S., Pawar, H.V., Tetteh, J., 2013. Polyox and carrageenan based composite film dressing containing anti-microbial and anti-inflammatory drugs for effective wound healing. Int. J. Pharm. 441, 181–191. https://doi.org/10.1016/j.ijpharm.2012.11.045.

Cambiaso-Daniel, J., Gallagher, J.J., Norbury, W.B., Finnerty, C.C., Herndon, D.N., Culnan, D.M., 2018. Treatment of Infection in Burn Patients. In: Total Burn Care. Elsevier, pp. 93–113.

Casariego, A., Souza, B.W.S., Cerqueira, M.A., Teixeira, J.A., Cruz, L., Díaz, R., Vicente, A.A., 2009. Chitosan/clay films' properties as affected by biopolymer and clay micro/nanoparticles' concentrations. Food Hydrocoll. 23, 1895–1902. https://doi.org/10.1016/j.foodhyd.2009.02.007.

Cern, A., Nativ-Roth, E., Goldblum, A., Barenholz, Y., 2014. Effect of solubilizing agents on Mupirocin loading into and release from PEGylated nanoliposomes. J. Pharm. Sci. 103, 2131–2138. https://doi.org/10.1002/jps.24037.

Dai, T., Tanaka, M., Huang, Y.-Y., Hamblin, M.R., 2011. Chitosan preparations for wounds and burns: antimicrobial and wound-healing effects. Expert Rev. Anti. Infect. Ther. 9, 857–879. https://doi.org/10.1586/eri.11.59.

Dang, Q., Liu, K., Liu, C., Xu, T., Yan, J., Yan, F., Cha, D., Zhang, Q., Cao, Y., 2018. Preparation, characterization, and evaluation of 3,6-O-N-acetylethylenediamine modified chitosan as potential antimicrobial wound dressing material. Carbohydr. Polym. 180, 1–12. https://doi.org/10.1016/j.carbpol.2017.10.019.

Deshmukh, P.T., Fernandes, J., Atul, A., Toppo, E., 2009. Wound healing activity of *Calotropis gigantea* root bark in rats. J. Ethnopharmacol. 125, 178–181. https://doi.org/10.1016/j.jep.2009.06.007.

Filippousi, M., Siafaka, P.I., Amanatiadou, E.P., Nanaki, S.G., Neratzaki, M., Bikiaris, D. N., Vizirianakis, I.S., Van Tendeloo, G., 2015. Modified chitosan coated mesoporous strontium hydroxyapatite nanorods as drug carriers. J. Mater. Chem. B 3, 5991–6000. https://doi.org/10.1039/C5TB00827A.

Finnerty, C.C., Jeschke, M.G., Branski, L.K., Barret, J.P., Dziewulski, P., Herndon, D.N., 2016. Hypertrophic scarring: the greatest unmet challenge after burn injury. Lancet (London, England) 388, 1427–1436. https://doi.org/10.1016/S0140-6736(16)31406-4.

Gal, A., Nussinovitch, A., 2009. Plasticizers in the manufacture of novel skin-bioadhesive patches. Int. J. Pharm. 370, 103–109. https://doi.org/10.1016/j.ijpharm.2008.11.015.

Ghosal, K., Chandra, A., Praveen, G., Snigdha, S., Roy, S., Agatemor, C., Thomas, S., Provaznik, I., 2018. Electrospinning over solvent casting: tuning of mechanical properties of membranes. Sci. Rep. 8, 5058. https://doi.org/10.1038/s41598-018-23378-3.

Gngr, S., Sedef, M., Zsoy, Y., 2012. Plasticizers in transdermal drug delivery systems. In: Luqman, Mohammad (Ed.), Recent Advances in Plasticizers. InTech.

Greaves, N.S., Ashcroft, K.J., Baguneid, M., Bayat, A., 2013. Current understanding of molecular and cellular mechanisms in fibroplasia and angiogenesis during acute wound healing. J. Dermatol. Sci. 72, 206–217. https://doi.org/10.1016/j.jdermsci.2013.07.008.

Grip, J., Engstad, R.E., Skjæveland, I., Škalko-Basnet, N., Holsæter, A.M., 2017. Sprayable Carbopol hydrogel with soluble beta-1,3/1,6-glucan as an active ingredient for wound healing – development and in-vivo evaluation. Eur. J. Pharm. Sci. 107, 24–31. https://doi.org/10.1016/j.ejps.2017.06.029.

Henry, B.D., Neill, D.R., Becker, K.A., Gore, S., Bricio-Moreno, L., Ziobro, R., Edwards, M.J., Mühlemann, K., Steinmann, J., Kleuser, B., Japtok, L., Luginbühl, M., Wolfmeier, H., Scherag, A., Gulbins, E., Kadioglu, A., Draeger, A., Babiychuk, E.B., 2014. Engineered liposomes sequester bacterial exotoxins and protect from severe invasive infections in mice. Nat. Biotechnol. 33, 81–88. https://doi.org/10.1038/nbt.3037.

Hima Bindu, T.V.L., Vidyavathi, M., Kavitha, K., Sastry, T.P., Suresh Kumar, R.V., 2010. Preparation and evaluation of chitosan-gelatin composite films for wound healing activity. Trends Biomater. Artif. Organs 24, 123–130.

Huang, M.-H., Yang, M.-C., 2009. Swelling and biocompatibility of sodium alginate/poly(γ -glutamic acid) hydrogels. Polym. Adv. Technol. 21, 561–567. https://doi.org/10.1002/pat.1466.

Hurler, J., Berg, O.L.E.A., Skar, M., Conradi, A.H., Al, P., Skalko-basnet, N.S.A., 2012. Improved burns therapy: liposomes-in-hydrogel delivery system for Mupirocin. J. Pharm. Sci. 1–10. https://doi.org/10.1002/jps.

Inukai, M., Jin, Y., Yomota, C., Yonese, M., Chethan, P.D., Vishalakshi, B., Sathish, L., Ananda, K., Poojary, B., Sun, K., Li, Z.H., Hye Kim, J., Il Kim, S., Kwon, I.B., Hyun Kim, M., Ik Lim, J., Novoa-Carballal, R., Müller, A.H.E., Xiaofeng Yu, Hunt, N.C., Grover, L.M., Guan, J., Dong, L.Z., Huang, S.J., Jing, M.L., Raafat, D., Fouad, G., Oungbho, K., Müller, B.W., Gupta, B., Saxena, S., Arora, A., Alam, M.S., Jana, S., Malakooty, E., Eslaminejad, M.B., Bagheri, F., Mollarazi, E., Gheibi, N., Khatri, N., Bilandi, A., Kataria, M.K., An, P., Issn, J., Krishnamoorthy, V., Priya, V., Prasad, R., Sen, S., Collins, M.N., Birkinshaw, C., Prestwich, G.D., Denkbas, E.B., Eroğlu, M., Irmak, S., Acar, A., Denkbaş, E.B., Oztürk, E., Ozdemir, N., Keçeci, K., Agalar, C., Fluid, S.B., López-Mata, M. a, Ruiz-Cruz, S., Silva-Beltrán, N.P., Ornelas-Paz, J.D.J., Zamudio-Flores, P.B., Burruel-Ibarra, S.E., Vilar, G., Tulla-Puche, J., Albericio, F., 2013. Chitosan-polyethylene glycol coated cotton membranes for wound dressings. Int. J. Pharm. 4, 342–361. https://doi.org/10.1016/j.ijbiomac.2013.04.045.

Jin, S.G., Yousaf, A.M., Kim, K.S., Kim, D.W., Kim, D.S., Kim, J.K., Yong, C.S., Youn, Y.S., Kim, J.O., Choi, H.-G., 2016. Influence of hydrophilic polymers on functional properties and wound healing efficacy of hydrocolloid based wound dressings. Int. J. Pharm. 501, 160–166. https://doi.org/10.1016/j.ijpharm.2016.01.044.

Kataria, K., Gupta, A., Rath, G., Mathur, R.B., Dhakate, S.R., 2014. In vivo wound healing performance of drug loaded electrospun composite nanofibers transdermal patch. Int. J. Pharm. 469, 102–110. https://doi.org/10.1016/j.ijpharm.2014.04.047.

Khalid, A., Khan, R., Ul-Islam, M., Khan, T., Wahid, F., 2017. Bacterial cellulose-zinc oxide nanocomposites as a novel dressing system for burn wounds. Carbohydr. Polym. 164, 214–221. https://doi.org/10.1016/j.carbpol.2017.01.061.

Kurczewska, J., Pecyna, P., Ratajczak, M., Gajęcka, M., Schroeder, G., 2017. Halloysite nanotubes as carriers of vancomycin in alginate-based wound dressing. Saudi Pharm. J. 25, 911–920. https://doi.org/10.1016/j.jsps.2017.02.007.

Kyzas, G.Z., Siafaka, P.I., Lambropoulou, D.A., Lazaridis, N.K., Bikiaris, D.N., 2013. Poly (itaconic acid)-Grafted Chitosan Adsorbents with Di ff erent Cross-Linking for Pb (II) and Cd (II) Uptake. https://doi.org/10.1021/la402778x.

Li, P., Dai, Y.-N., Zhang, J.-P., Wang, A.-Q., Wei, Q., 2008. Chitosan-alginate nanoparticles as a novel drug delivery system for nifedipine. Int. J. Biomed. Sci. 4, 221–228.

Li, S., Li, L., Guo, C., Qin, H., Yu, X., 2017. A promising wound dressing material with excellent cytocompatibility and proangiogenesis action for wound healing: Strontium loaded Silk fibroin/Sodium alginate (SF/SA) blend films. Int. J. Biol. Macromol. 104, 969–978. https://doi.org/10.1016/j.ijbiomac.2017.07.020.

Lim, H., Hoag, S.W., 2013. Plasticizer effects on physical-mechanical properties of solvent cast Soluplus® films. AAPS PharmSciTech 14, 903–910. https://doi.org/10.1208/s12249-013-9971-z.

López-Mata, M.A., Ruiz-Cruz, S., Silva-Beltrán, N.P., Ornelas-Paz, J.D.J., Ocaño-Higuera, V.M., Rodríguez-Félix, F., Cira-Chávez, L.A., Del-Toro-Sánchez, C.L., Shirai, K., 2015. Physicochemical and antioxidant properties of chitosan films incorporated with cinnamon oil. Int. J. Polym. Sci. 2015. https://doi.org/10.1155/2015/974506.

Lozano-Navarro, J., Díaz-Zavala, N., Velasco-Santos, C., Melo-Banda, J., Páramo-García, U., Paraguay-Delgado, F., García-Alamilla, R., Martínez-Hernández, A., Zapién-Castillo, S., 2018. Chitosan-starch films with natural extracts: physical, chemical, morphological and thermal properties. Materials (Basel) 11, 120. https://doi.org/10.3390/ma11010120.

Ma, Y., Xin, L., Tan, H., Fan, M., Li, J., Jia, Y., Ling, Z., Chen, Y., Hu, X., 2017. Chitosan membrane dressings toughened by glycerol to load antibacterial drugs for wound healing. Mater. Sci. Eng. C 81, 522–531. https://doi.org/10.1016/j.msec.2017.08.052.

Maria, V.D., Bernal, C., Francois, N.J., 2016. Development of Biodegradable Films Based on Chitosan/Glycerol Blends Suitable for Biomedical Applications. J. Tissue Sci. Eng. 07. https://doi.org/10.4172/2157-7552.1000187.

Mohamad, N., Mohd Amin, M.C.I., Pandey, M., Ahmad, N., Rajab, N.F., 2014. Bacterial cellulose/acrylic acid hydrogel synthesized via electron beam irradiation: accelerated burn wound healing in an animal model. Carbohydr. Polym. 114, 312–320. https://doi.org/10.1016/j.carbpol.2014.08.025.

Mpharm, K.D., Ramana, M.V., Sara, U.V.S., Agrawal, D.K., Mpharm, K.P., Chakravarthi, S., 2010. Preparation and evaluation of transdermal plasters containing norfloxacin: a novel treatment for burn wound healing. Eplasty 10, e44.

Murakami, K., Aoki, H., Nakamura, S., Nakamura, S.I., Takikawa, M., Hanzawa, M., Kishimoto, S., Hattori, H., Tanaka, Y., Kiyosawa, T., Sato, Y., Ishihara, M., 2010. Hydrogel blends of chitin/chitosan, fucoidan and alginate as healing-impaired wound dressings. Biomaterials 31, 83–90. https://doi.org/10.1016/j.biomaterials.2009.09.031.

Nilani, P., Pranavi, A., Duraisamy, B., Damodaran, P., Subhashini, V., Elango, K., 2011. Formulation and evaluation of wound healing dermal patch. African J. Pharm. Pharmacol. 5, 1252–1257. https://doi.org/10.5897/AJPP11.467.

Okur, M.E., Ayla, Ş., Çiçek-Polat, D., Günal, M.Y., Yoltaş, A., Biçeroğlu, Ö., 2018. Novel insight into wound healing properties of methanol extract of *Capparis ovata* Desf. var. *palaestina* Zoh. fruits. J. Pharm. Pharmacol., 1–13 https://doi.org/10.1111/jphp.12977.

Pawar, H.V., Tetteh, J., Boateng, J.S., 2013. Preparation, optimisation and characterisation of novel wound healing film dressings loaded with streptomycin and diclofenac. Colloids Surfaces B Biointerfaces 102, 102–110. https://doi.org/10.1016/j.colsurfb.2012.08.014.

Peh, K.K., Wong, C.F., 1999. Polymeric films as vehicle for buccal delivery: swelling, mechanical, and bioadhesive properties. J. Pharm. Pharm. Sci. 2, 53–61.

Pereda, M., Ponce, A.G., Marcovich, N.E., Ruseckaite, R.A., Martucci, J.F., 2011. Chitosan-gelatin composites and bi-layer films with potential antimicrobial activity. Food Hydrocoll. 25, 1372–1381. https://doi.org/10.1016/j.foodhyd.2011.01.001.

Pereira, R., Carvalho, A., Vaz, D.C., Gil, M.H., Mendes, A., Bártolo, P., 2013. Development of novel alginate based hydrogel films for wound healing applications. Int. J. Biol. Macromol. 52, 221–230. https://doi.org/10.1016/j.ijbiomac.2012.09.031.

Perumal, S., Ramadass, S.K., Madhan, B., 2014. Sol – gel processed mupirocin silica microspheres loaded collagen scaffold: a synergistic bio-composite for wound healing. Eur. J. Pharm. Sci. 52, 26–33. https://doi.org/10.1016/j.ejps.2013.10.006.

Prateepchanachai, S., Thakhiew, W., Devahastin, S., Soponronnarit, S., 2017. Mechanical properties improvement of chitosan films via the use of plasticizer, charge modifying agent and film solution homogenization. Carbohydr. Polym. 174, 253–261. https://doi.org/10.1016/j.carbpol.2017.06.069.

Priyadarshi, R., Sauraj, Kumar, B., Negi, Y.S., 2018. Chitosan film incorporated with citric acid and glycerol as an active packaging material for extension of green chilli shelf life. Carbohydr. Polym. 195, 329–338. https://doi.org/10.1016/j.carbpol.2018.04.089.

Pu-you, J., Cai-ying, B., Li-hong, H., Yong-hong, Z., 2014. Properties of poly(vinyl alcohol) plasticized by glycerin. J. For. Prod. Ind. 3, 151–153.

Rahman, M., Brazel, C., 2004. The plasticizer market: an assessment of traditional plasticizers and research trends to meet new challenges. Prog. Polym. Sci. 29, 1223–1248. https://doi.org/10.1016/j.progpolymsci.2004.10.001.

Raval, J.P., Naik, D.R., Patel, P.S., 2011. Preparation and evaluation of gatifloxacin dermal patches as wound dressing. Int. J. Drug Formul. Res., 247–259

Ravichandiran, V., Manivannan, S., 2015. Wound healing potential of transdermal patches containing bioactive fraction from the bark of *Ficus racemosa*. Int. J. Pharm. Pharm. Sci. 7, 326–332.

Rippon, M., White, R., Davies, P., 2007. Skin adhesives and their role in wound dressings. Wounds UK 3, 76–86.

Schmidt, P., Dybal, J., Šturcová, A., 2009. ATR FTIR investigation of interactions and temperature transitions of poly(ethylene oxide), poly(propylene oxide) and ethylene oxide-propylene oxide-ethylene oxide tri-block copolymers in water media. Vib. Spectrosc. 50, 218–225. https://doi.org/10.1016/j.vibspec.2008.12.003.

Serra, M.B., Barroso, W.A., Silva, N.N.Da., Silva, S.D.N., Borges, A.C.R., Abreu, I.C., Borges, M.O.D.R., 2017. From inflammation to current and alternative therapies involved in wound healing. Int. J. Inflam. 2017. https://doi.org/10.1155/2017/3406215.

Sezer, A.D., Hatipoglu, F., Cevher, E., Oğurtan, Z., Bas, A.L., Akbuğa, J., 2007. Chitosan film containing fucoidan as a wound dressing for dermal burn healing: Preparation and in vitro/in vivo evaluation. AAPS PharmSciTech 8, E94–E101. https://doi.org/10.1208/pt0802039.

Shaw, T.J., Martin, P., 2009. Wound repair at a glance. J. Cell Sci. 122, 3209–3213. https://doi.org/10.1242/jcs.031187.

Siafaka, P., Üstündağ Okur, N., Mone, M., Giannakopoulou, S., Er, S., Pavlidou, E., Karavas, E., Bikiaris, D., 2016a. Two different approaches for oral administration of voriconazole loaded formulations: electrospun fibers versus β-cyclodextrin complexes. Int. J. Mol. Sci. 17, 282. https://doi.org/10.3390/ijms17030282.

Siafaka, P.I., Barmbalexis, P., Bikiaris, D.N., 2016b. Novel electrospun nanofibrous matrices prepared from poly(lactic acid)/poly(butylene adipate) blends for controlled release formulations of an anti-rheumatoid agent. Eur. J. Pharm. Sci. 88, 12–25. https://doi.org/10.1016/j.ejps.2016.03.021.

Siafaka, P.I., Barmpalexis, P., Lazaridou, M., Papageorgiou, G.Z., Koutris, E., Karavas, E., Kostoglou, M., Bikiaris, D.N., 2015a. Controlled release formulations of risperidone antipsychotic drug in novel aliphatic polyester carriers: Data analysis and modelling. Eur. J. Pharm. Biopharm. 94, 473–484. https://doi.org/10.1016/j.ejpb.2015.06.027.

Siafaka, P.I., Mone, M., Koliakou, I.G., Kyzas, G.Z., Bikiaris, D.N., 2016c. Synthesis and physicochemical properties of a new biocompatible chitosan grafted with 5-hydroxymethylfurfural. J. Mol. Liq. 222, 268–271. https://doi.org/10.1016/j.molliq.2016.07.027.

Siafaka, P.I., Titopoulou, A., Koukaras, E.N., Kostoglou, M., Koutris, E., Karavas, E., Bikiaris, D.N., 2015b. Chitosan derivatives as effective nanocarriers for ocular release of timolol drug. Int. J. Pharm. 495, 249–264. https://doi.org/10.1016/j.ijpharm.2015.08.100.

Siafaka, P.I., Zisi, A.P., Exindari, M.K., Karantas, I.D., Bikiaris, D.N., 2016d. Porous dressings of modified chitosan with poly(2-hydroxyethyl acrylate) for topical wound delivery of levofloxacin. Carbohydr. Polym. 143, 90–99. https://doi.org/10.1016/j.carbpol.2016.02.009.

Singh, B., Sharma, A., Sharma, A., Dhiman, A., 2017a. Design of antibiotic drug loaded carbopol- hydrogel for wound dressing applications. Am. J. Drug Deliv. Ther. 4, 1–9.

Singh, B., Sharma, S., Dhiman, A., 2013. Design of antibiotic containing hydrogel wound dressings: biomedical properties and histological study of wound healing. Int. J. Pharm. 457, 82–91. https://doi.org/10.1016/j.ijpharm.2013.09.028.

Singh, S., Young, A., McNaught, C.E., 2017b. The physiology of wound healing. Surg. (United Kingdom) 35, 473–477. https://doi.org/10.1016/j.mpsur.2017.06.004.

Tanwar, Y.S., 2005. Formulation and evaluation of transdermal films of salbutamol sulfate. Dhaka Univ. J. Pharm. Sci. 4, 93–97.

Tomczykowa, M., Wróblewska, M., Winnicka, K., Wieczorek, P., Majewski, P., Celińska-Janowicz, K., Sawczuk, R., Miltyk, W., Tryniszewska, E., Tomczyk, M., 2018. Novel gel formulations as topical carriers for the essential oil of bidens tripartita for the treatment of candidiasis. Molecules 23, 2517. https://doi.org/10.3390/molecules23102517.

Üstündağ-Okur, N., Gökçe, E.H., Bozbıyık, D.İ., Eğrilmez, S., Ertan, G., Özer, Ö., 2015. Novel nanostructured lipid carrier-based inserts for controlled ocular drug delivery: evaluation of corneal bioavailability and treatment efficacy in bacterial keratitis. Expert Opin. Drug Deliv. 12, 1791–1807. https://doi.org/10.1517/17425247.2015.1059419.

Üstündag-Okur, N., Gökçe, E.H., Eğrilmez, S., Özer, Ö., Ertan, G., 2014. Novel ofloxacin-loaded microemulsion formulations for ocular delivery. J. Ocul. Pharmacol. Ther. 30, 319–332. https://doi.org/10.1089/jop.2013.0114.

Üstündağ Okur, N., Filippousi, M., Okur, M.E., Ayla, Ş., Çağlar, E.Ş., Yoltaş, A., Siafaka, P.I., 2018. A novel approach for skin infections: controlled release topical mats of poly(lactic acid)/poly(ethylene succinate) blends containing Voriconazole. J. Drug Deliv. Sci. Technol. 46, 74–86. https://doi.org/10.1016/j.jddst.2018.05.005.

Wang, P.H., Huang, B.S., Horng, H.C., Yeh, C.C., Chen, Y.J., 2018. Wound healing. J. Chinese Med. Assoc. 81, 94–101. https://doi.org/10.1016/j.jcma.2017.11.002.

Yasasvini, S., Anusa, R.S., VedhaHari, B.N., Prabhu, P.C., RamyaDevi, D., 2017. Topical hydrogel matrix loaded with Simvastatin microparticles for enhanced wound healing activity. Mater. Sci. Eng., C 72, 160–167. https://doi.org/10.1016/j.msec.2016.11.038.

Zhang, L., Ma, Y., Pan, X., Chen, S., Zhuang, H., Wang, S., 2018. A composite hydrogel of chitosan/heparin/poly (γ-glutamic acid) loaded with superoxide dismutase for wound healing. Carbohydr. Polym. 180, 168–174. https://doi.org/10.1016/j.carbpol.2017.10.036.

Zhou, X., Wang, H., Zhang, J., Li, X., Wu, Y., Wei, Y., Ji, S., Kong, D., Zhao, Q., 2017. Functional poly(ε-caprolactone)/chitosan dressings with nitric oxide-releasing property improve wound healing. Acta Biomater. 54, 128–137. https://doi.org/10.1016/j.actbio.2017.03.011.